Geotechnical Aspects of Underground Construction in Soft Ground – Yoo, Park, Kim & Ban (Eds)

Effect of soil-basement interaction on seismic responses of structures

D.K. Kim
Dankook University, Korea

D.S. Kim & H.G. Ha
Korea Advanced Institute of Science and Technology, Korea

ABSTRACT: In order to investigate the effect of soil-basement interaction on the earthquake response of structure, centrifuge tests were performed using an in-flight earthquake simulator. The test specimen was composed of a single-degree-of-freedom structure model, a substructure model, and soil deposit in a centrifuge container. The earthquake responses of the fixed and embedded basements depended on those of the massive soil deposit. Not only the ground motion but also the inertia force of the basement, which was in the forced vibration by the massive soil deposit, amplified the seismic loads of the structures. The seismic loads of the structures on the half-embedded basement were greater than those of the fixed base structures in whole period range. When the maximum dynamic earth pressure acted on the front side of the basement during the earthquake, the earth pressures on the opposite side of the basement were diminished due to the gap between the soil and the basement.

1 INTRODUCTION

Recently it has been generalized to perform the nonlinear static analysis (Pushover) or the nonlinear time history analysis for the performance based seismic design of structure. In most analysis procedures focusing on the behavior of structure, the amplified excitation by the soil deposit is imposed to the fixed base of structure regardless of the basements. However, for reasonable seismic design, actual substructures (e.g. shallow foundation, deep basement, and pier group), which support the structure and interact with the soil deposit, should be included in the seismic analysis procedures.

However, it has been uncertain to determine role of basement during the earthquake. When the basement was fixed to the bedrock due to the shallow soil deposit, base level for site classification and corresponding site amplification factor have been in controversy. There were two assumptions in practical design phase (Kim 2007). Firstly, because the basement was considered as a relatively stiff structure than the soil deposit, the near soil deposit was neglected. Thus, the base level for site classification was the bottom of basement. Secondly, because the soil deposit was very massive, the stiffness of basement was neglected. Thus, the base level for site classification was the ground surface. Also, when the soil deposit was deep and the basement was not fixed to the bedrock, the ground motion can be reduced to foundation input motion due to the embedment effect of basement in FEMA 440 (2004).

The present study focuses on the effect of soil-basement interaction on the earthquake response of structure, and centrifuge tests were performed. During the centrifuge tests, the earthquake response of structures on the box-shaped basements in the soil deposit was investigated, using an in-flight earthquake simulator. A fixed basement to the bottom of ESB box was used. Also, an embedded basement model was used to observe the embedment effect. Four SDOF structure models with various periods were used to evaluate the seismic load of the structure on the basement. Changing the centrifugal acceleration level and the type and peak level of input earthquake accelerations, the earthquake responses of soil deposit, basement, and structure were observed.

2 TEST PROGRAM

The test specimen comprised soil deposit, a basement, and a Single-Degree-of-Freedom (SDOF) structure model in a soil container. Figure 1(a)∼Figure 1(c) show construction of the test specimen. The soil container used in this study is the Equivalent Shear Beam (ESB) type, which is composed of shear beam boxes so that the horizontal movement of the soil is able to reduce the reflection of the waves at the boundary of the container (Zeng & Schofield 1996, Lee et al. 2013). The container is mounted on a horizontal shaking table attached to the centrifuge apparatus (Kim et al. 2013). The external and internal dimensions of the soil container were 0.6 m × 0.6 m × 0.63 m, and 0.49 m × 0.49 m × 0.6 m (length × width × depth), respectively. In 60 g centrifugal acceleration the size of the equivalent prototype soil corresponds to 29.4 m × 29.4 m × 36 m.

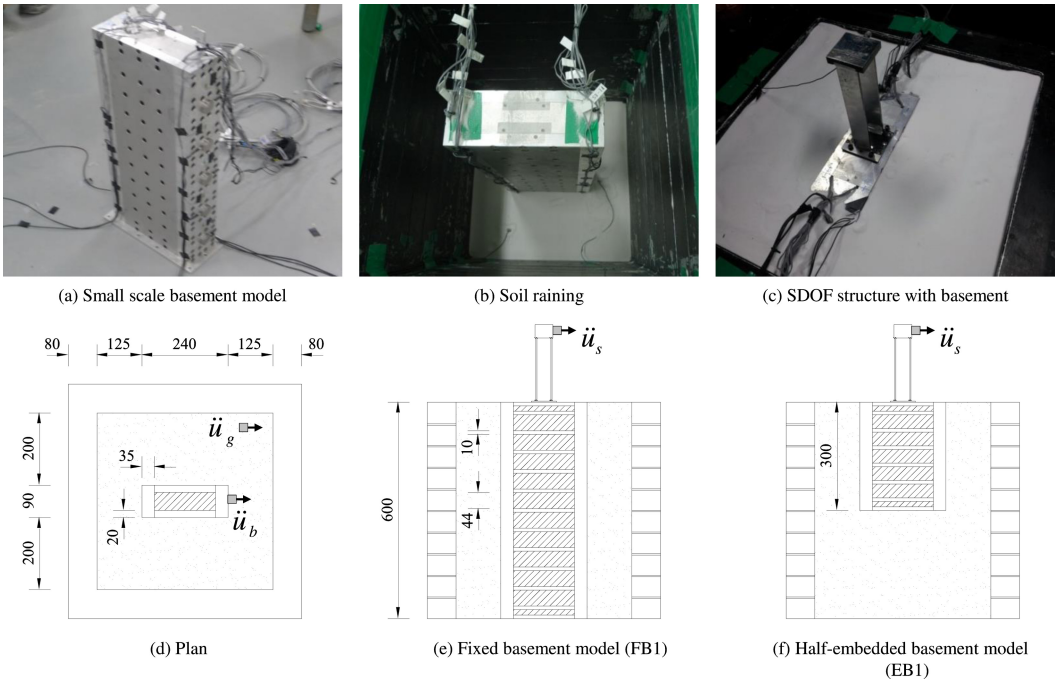

Figure 1. Test specimen.

2.1 *Soil properties*

The silica-sand layers were arranged in the container by a sand-rainer to have 80% relative density. The sand layers of all the centrifuge tests were in dry condition. The shear-wave velocities of the soil strata were measured by an in-flight bender element array under centrifugal acceleration (Kim & Kim 2010). The elastic site period, T_{soil}, of the prototype soil was estimated as 0.26 s in 20 gc, 0.41 s in 40 gc and 0.56 s in 60 gc using the following equation (Kramer 1996).

$$T_{soil} = 4\sum_{i=1}^{n} \frac{D_i}{V_{Si}} \tag{1}$$

where D_i and V_{Si} are the thickness and the shear-wave velocity of each soil layer, respectively and n is the total number of layers.

2.2 *Basement models*

Figure 1(d)~Figure 1(f) show the small-scale basement model in this test. The size of basement was 240 × 90 mm, and that of the prototype in 60 g centrifugal acceleration was 14.4 × 5.4 m. The small-scale basement was made of aluminum. The thicknesses of exterior walls of the basement were 35 mm and 20 mm. The walls were connected by 10 mm horizontal plates with bolting. Figure 1(e) shows a fixed basement model (FB1), and the depth of the fixed basement was 600 mm and the same as the depth of the soil deposits. To investigate the effect of soil deposits on the earthquake responses of the structures with the fixed basement, the existence of the soil deposits was the test variable. Thus, the centrifuge tests in the case of the fixed basement without the soil deposits were performed. Figure 1(f) shows a half-embedded basement (EB1) with the same plan of the fixed basement.

From the centrifuge tests for the fixed basement without the soil deposits, the natural periods, T_b, of the basement could be estimate as 0.15 s, 0.27 s, and 0.35 s in 20 g, 40 g, and 60 g centrifugal acceleration, respectively.

The weight of the fixed basement was 28.1 kg, 1.26 times that of the same volume of soil. And the weight of the half-embedded basement was 14.4 kg, 1.29 times that of the same volume of soil.

Using Equation 2 and ratios of the site periods, T_{soil}, to the estimated periods, T_b, of basement, stiffness ratios of the basement to the soil deposits were estimated as 3.8, 2.9, and 2.9 in 20 g, 40 g, and 60 g centrifugal acceleration. This indicates that the stiffness of the basement was relatively greater than that of the same volume of soil.

$$\frac{k_{b,1}}{k_{soil,1}} = \left(\frac{m_{b,1}}{m_{soil,1}}\right) \times \left(\frac{T_{soil,1}}{T_{b,1}}\right)^2 \tag{2}$$

where $m_{b,1}/m_{soil,1}$: the mass ratio of the basement to the soil deposit with the same dimension for the first mode, $T_{soil,1}/T_{b,1}$: ratio of the period of the soil deposit to that of the basement for the first mode.

Table 1. Properties of structure models.

	SDOF-1	SDOF-2	SDOF-3	SDOF-4
Effective mass (kg)	0.211	0.265	0.792	1.272
Effective stiffness (kN/m)	424.6	60.5	60.5	20.1
T_n[1)] in 20 gc[2)]	0.09	0.26	0.45	1.00
T_n in 40 gc	0.18	0.52	0.90	2.00
T_n in 60 gc	0.27	0.78	1.35	3.00
Damping ratio	0.009	0.022	0.014	0.021

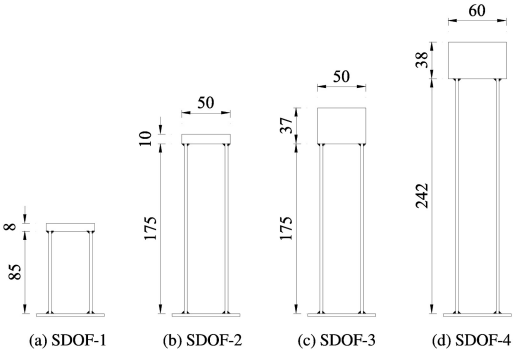

Figure 2. Superstructure models.

2.3 *Structure model*

To investigate the earthquake responses of the structures on the basements, the natural period of the structure was a variable in the present study. The structures were Single-Degree-of-Freedom (SDOF) structures made of steel, and composed of two steel plates and a lumped mass. The two steel plates connected the lumped mass and the base plate by welding, and the base plate of the SDOF structure was connected to the top of the basement by bolting.

Kim & Yoon (2006) about the site response analysis reported that the responses of structures were significantly amplified by the resonance between the structure and the site. Thus, on the basis of the site period, the natural periods of the SDOF structures were calibrated by changing the length of the steel plates and the lumped mass.

In 1 g gravity field, the natural periods of the small-scale structure models were measured by performing impact hammer testing and FFT analysis for the test results. The damping ratios of the structure models were estimated from the decay of the dynamic response after impact loading.

Figure 2 shows the dimensions of structure models and Table 1 presents the effective stiffness and the effective mass of the small-scale structure models in 1g and the dynamic periods of the prototype structures corresponding to 20 g, 40 g and 60 g centrifugal accelerations.

2.4 *Input accelerations*

Four earthquake accelerations were applied to the base of ESB box. From the PEER Ground Motion Database, the earthquake motions, which were recorded at rock sites, were selected as the input motions (the 1971 San Fernando earthquake, the 1984 Morgan Hill earthquake, the 1994 Northridge earthquake, and the 1995 Kobe earthquake). To investigate dynamic periods of the soil and the basements, a sine sweep wave was used. During staged testing, the levels of the base excitation accelerations were gradually increased from 0.045 g to 0.46 g.

3 TIME HISTORY RESPONSES

3.1 *Displacement time history responses of basements*

To observe effects of the soil deposit on earthquake responses of the basements, displacement time history responses of the basements in the soil deposit were compared with those of the basement without the soil deposit. Figure 3 shows the displacement time history responses of the soil and the basements in 20 g centrifugal acceleration. The input earthquake was the Northridge earthquake, and the effective peak ground accelerations (EPGA) of the input motions were estimated as 0.27 g. The measured accelerations of the soil deposit and the basement ($\ddot{u}_g$ and $\ddot{u}_b$ in Figure 1(d)) were converted to the displacements using a high-pass filter and a double integration method to prevent the divergence of the integration of the measured acceleration. The cut-off frequency for the high-pass filter was 0.5 Hz.

The stiffness of FB1 was 3.75 times that of the soil deposit. Even though the weight of FB1 was 25% greater than that of the soil deposit, the dynamic period of FB1 was smaller than that of the nonlinear soil deposit as 0.15 s. Thus, the maximum displacements of FB1 without the soil deposit were only 5.4 mm in Figure 3(a-1). However, when the FB1 was in the soil deposit, the maximum displacement of FB1 was increased to 8.8 mm due to inertia of the massive soil deposit in Figure 3(a-2). This indicates that even though the stiff basement was fixed to the bedrock, the earthquake behavior of the basement depends on that of the massive soil deposit. However, the maximum displacement of FB1 was 90% of those of the ground motion due to the large stiffness of the basement.

For the EB1, which was a half-embedded basement, Figure 3(b) compares the displacement time history responses of the ground motion and the EB1. Like the earthquake response of the FB1, the earthquake response of the EB1 depended on that of the massive soil deposit. Thus, the maximum amplitudes of the two time history responses of the ground motion and the EB1 were almost identical. This indicates that when the basement was not fixed to the bedrock and embedded, the embedded basement floated in and moved with the soil deposit due to the inertia of massive soil deposit.

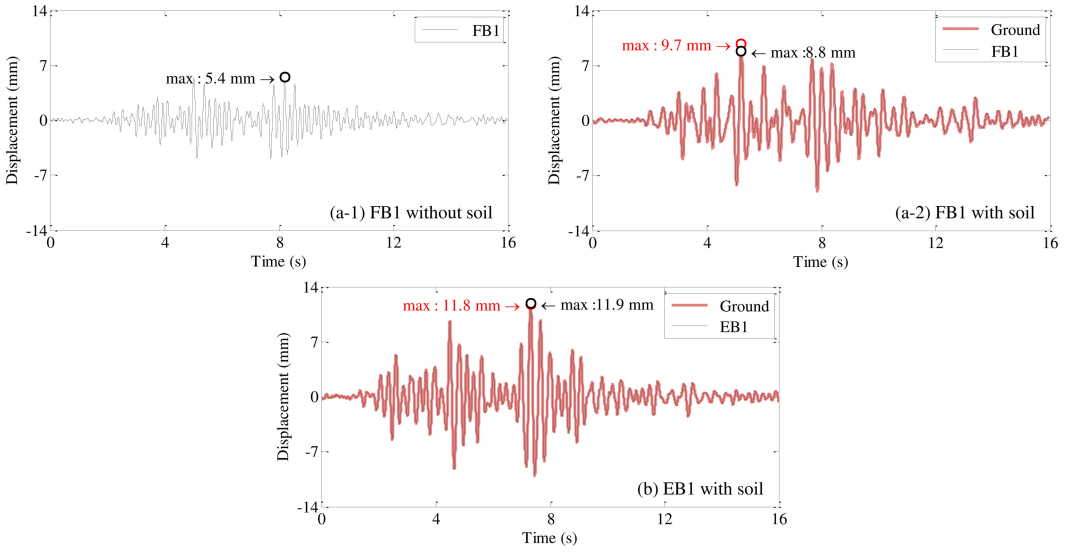

Figure 3. Acceleration time history responses of fixed and embedded substructures.

3.2 *Acceleration time history responses of structures*

To observe the earthquake response of the structure on the basement, the horizontal acceleration, $\ddot{u}_s$, at the top of the structure was measured in Figure 1(e) and Figure 1(f). Also, the total acceleration, $\ddot{u}_t$, of the fixed base structure model using the measured acceleration, $\ddot{u}_g$, at the ground surface was calculated.

On the basis of the total response, u_t, of the fixed base structure model, Equation 3 shows the equation of motion.

$$m_s\ddot{u}_t + c_s(\dot{u}_t - \dot{u}_g) + k_s(u_t - u_g) = 0 \tag{3}$$

where m_s, c_s, and k_s are the mass, damping coefficient, and stiffness of the structure and presented in Table 1. The seismic load of the structure can be calculated as $k_s(u_t - u_g)$. In Table 1, the damping ratios of the structures were smaller than 2.5%, which indicates that the damping effect on the seismic load of the structure were negligible. Thus, on the basis of Equation (4), the total acceleration, $\ddot{u}_t$, including the accelerations of the ground motion and the structure can be considered as the acceleration representing the seismic load of structure.

$$\ddot{u}_t = -\frac{1}{m_s}\left(c_s\left(\dot{u}_t - \dot{u}_g\right) + k_s\left(u_t - u_g\right)\right) \tag{4}$$

In the same context, the measured acceleration, $\ddot{u}_s$, at the top of structure can be considered as the seismic load of the structure during the centrifuge test. Thus, from the comparison between the total accelerations of the structure on the basement and the fixed base structure, the effect of the basement on the seismic load of the structure was investigated.

Figure 4 shows acceleration time history responses of the structures on the basements in the soil deposit and the fixed base structure model. The input earthquake was the Northridge earthquake, and the effective peak ground accelerations (EPGA) of the input motions were estimated as 0.27 g.

For the SDOF-1, because the fixed basement (FB1) reduced the high frequency components of the ground motion, the seismic load of the structure on the basements were decreased in comparison with that of the fixed base structure. On the other hand, the embedded basement (EB1) amplified the seismic load of SDOF-1 to 1.63 times of that of the fixed base structure.

For SDOF-2 with period of 0.26 s, which was similar to the site period ($T_{soil} = 0.26$ s) in 20 g centrifugal acceleration, Figure 4(a-2) shows the earthquake responses of SDOF-2. Generally, it has been known that the earthquake responses of structures are significantly amplified by the resonance between the soil deposit and the structure (Kim & Yoon). Thus, the measured accelerations at the ground surface were amplified by the characteristics of the soil deposit. Also, the amplified accelerations affected the seismic loads of the fixed base structure in Figure 4(a-2) and Figure 4(b-2). Nevertheless, the seismic loads of SDOF-2 on the basements (FB1 and EB1) were 27% and 54% greater than those of the fixed base structure. This indicates that the basements as well as the soil deposit might amplify the seismic load of the structure.

Like the response amplification of SDOF-2, the seismic loads of SDOF-3 with period of 0.45 s were amplified by not only the soil deposit but also the basement in Figure 4(a-3) and Figure 4(b-3). The seismic loads of SDOF-3 on the basements were 26% and 21% greater than those of the fixed base structure.

In Figure 4(a-4) and Figure 4(b-4), the earthquake responses of SDOF-4 with period of 1.00 s were compared with those of the fixed base structure. When SDOF-4 was on the embedded basement (EB1), the earthquake responses of SDOF-4 were similar to those

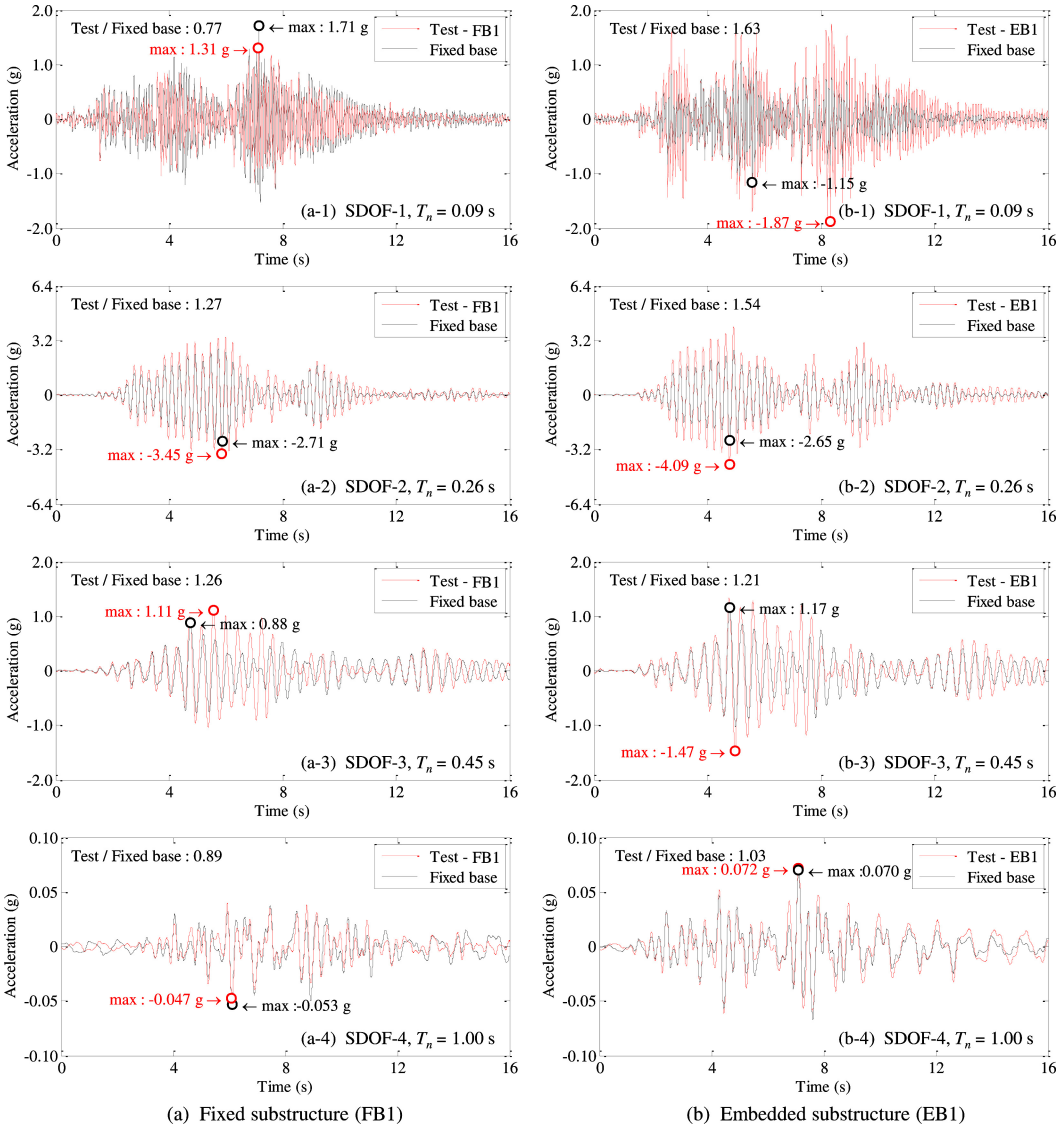

Figure 4. Acceleration time history responses of superstructures on substructures.

of the fixed base structure. Because the period of SDOF-4 was apart from the site period, the both amplifications by the soil deposits and the basements were small. On the other hand, the seismic load of SDOF-4 on the stiff basement (FB1) was 89% of those of the fixed base structure. As shown in Figure 3(a-2), this is because the response amplitude of the basement were reduced by the stiffness of basement, which was 3.75 times of those of the soil deposit.

4 SEISMIC LOAD

Figure 5 compares the seismic loads of the structures on the basements with those of the fixed base structures. In Figure 4(a-2), the maximum displacement of the stiff basement (FB1) was 90% of those of the ground motion. However, the seismic loads of the structures (SDOF-2 and SDOF-3) on the stiff basement were 28%～61% greater than those of the fixed base model. In other word, even though the earthquake behaviors of the basement were slightly reduced by the kinematic interaction between the stiff basement and the soil deposit, the seismic loads of the structures were amplified by the basements. This means that the structure and the basement should be simultaneously considered in the seismic analysis and design procedure. For the long-period structure (SDOF-4), the seismic loads of the structure were similar to those of the fixed base structure.

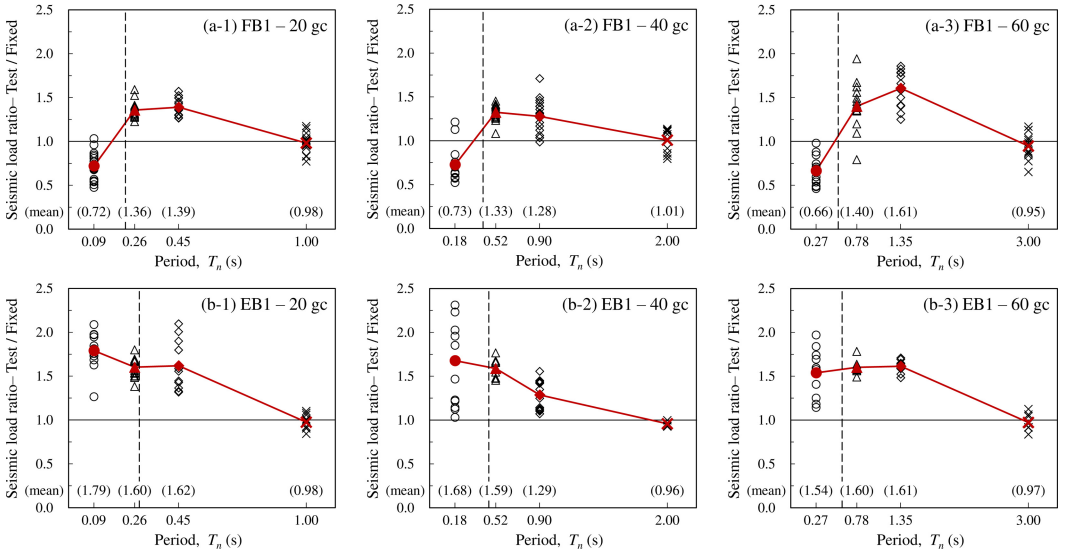

Figure 5. Seismic load ratio of superstructure on substructure to fixed base model.

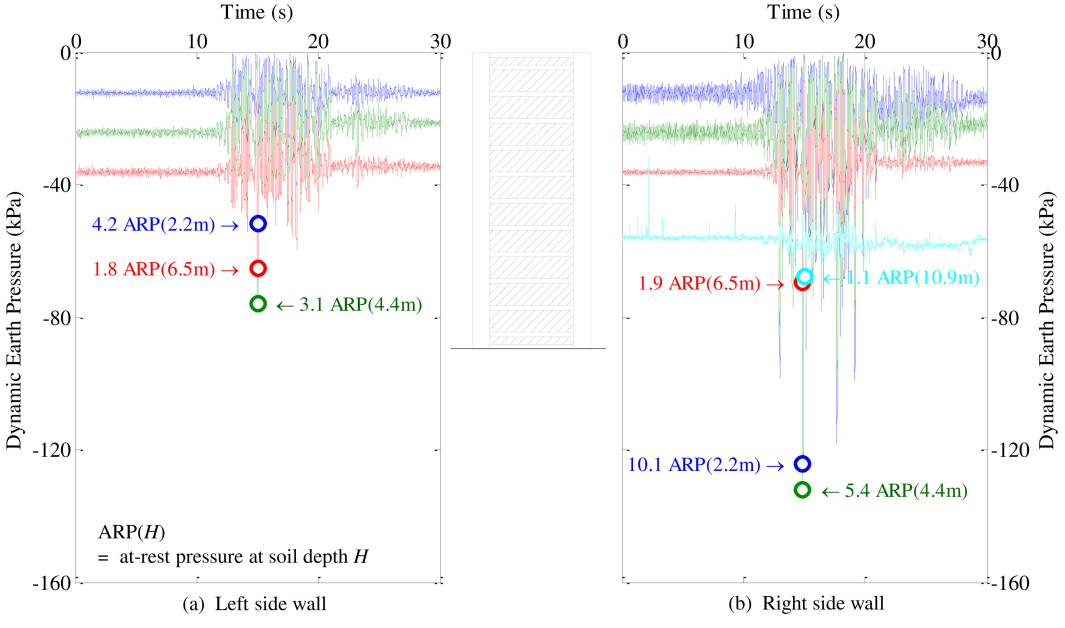

Figure 6. Time history responses of dynamic earth pressure (Northridge earthquake (Input PGA ≒ 0.16 g), Soil depth = 12 m in 20 gc.

The seismic loads of the structures on the half-embedded basement (EB1) were greater than those of the fixed base structures in whole period range.

5 EARTH PRESSURE

As the basement has not been considered in the seismic design procedure, dynamic earth pressure due to the earthquake has been ignored, too. On the other hand, it has been assumed that when the dynamic earth pressure acts on the front side of the basement during the earthquake, the lateral soil force by the earthquake might be offset by the at-rest earth pressure on the opposite side of the basement (Kim 2007). However, data for the dynamic earth pressure on the basement were few to investigate effects of the dynamic earth pressure.

In this study, the dynamic earth pressure on the basement was observed from the centrifuge test. As the centrifuge can simulate actual stress of the soil deposits by N g centrifugal acceleration, reasonable earth

pressure can be investigated. The observed dynamic earth pressure was compared with the at-rest earth pressure.

5.1 *Time history response*

Figure 6 shows time history responses of dynamic earth pressures acting on the fixed basement (FB1). In 20 g centrifugal acceleration, the depth of the prototype soil deposit was 12 m and the site period was 0.26 s. The input motion was Northridge acceleration and the peak of the input earthquake acceleration was 0.16 g.

As mentioned above, the at-rest earth pressures act on the basement before the earthquake. Thus, the measured earth pressures before the earthquake were calibrated to the corresponding the at-rest earth pressures (hearafter ARP(z_i)), which were increased by the depth z_i from the surface.

Contrary to the at-rest earth pressure, the measured dynamic earth pressures near the surface were significantly greater than those near the bedrock during the earthquake. Also, the measured dynamic earth pressure was 10 times of the at-rest earth pressure at the depth of 2.2 m from the surface ARP (2.2 m). This indicates that the exterior wall near the surface resisting only the very small at-rest earth pressure can be significantly damaged by the dynamic earth pressure rather than the exterior wall near the bed rock resisting the large at-rest earth pressure.

5.2 *Dynamic earth pressure profile*

Figure 7 shows dynamic earth pressure profiles at maximum pressure acting on each side. When the maximum dynamic earth pressure acted on the front side of the basement, the earth pressures on the opposite side of basement were diminished due to the gap between the soil and the basement. This means that the at-rest earth pressure on the opposite side is not effective to resist the lateral soil force.

Thus, as shown in Figure 7, the basement should be designed for the dynamic earth pressure acting on the front side without considering the at-rest earth pressure on the opposite side. Also, it is recommended to use envelope of the dynamic earth pressure profiles for the safe seismic design.

As the levels of input accelerations increased, the free-field motions increased. Thus, the dynamic earth pressures increased depending on the input peak accelerations. Figure 8 shows dynamic earth pressure profiles according to the input peak accelerations.

When the input peak accelerations were smaller than 0.1 g, the dynamic earth pressure were similar to the at-rest earth pressures due to small displacements of the soil deposits. However, as the input peak accelerations increased, the dynamic earth pressures were significantly greater than the at-rest earth pressures. Also, even though the at-rest earth pressures near the surface were smaller than those near the bedrock,

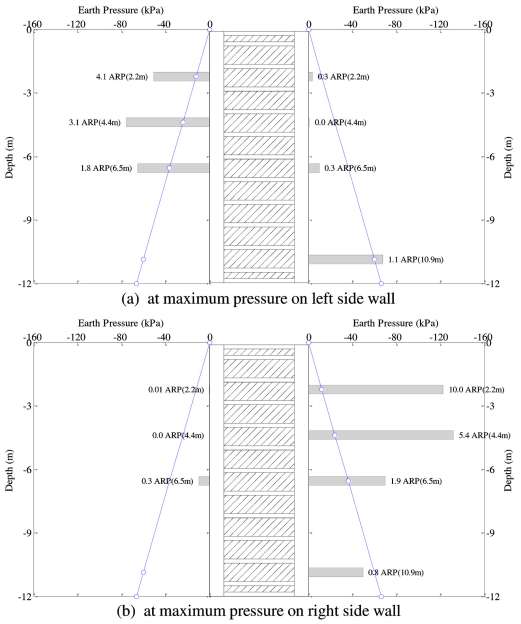

Figure 7. Dynamic earth pressure profile.

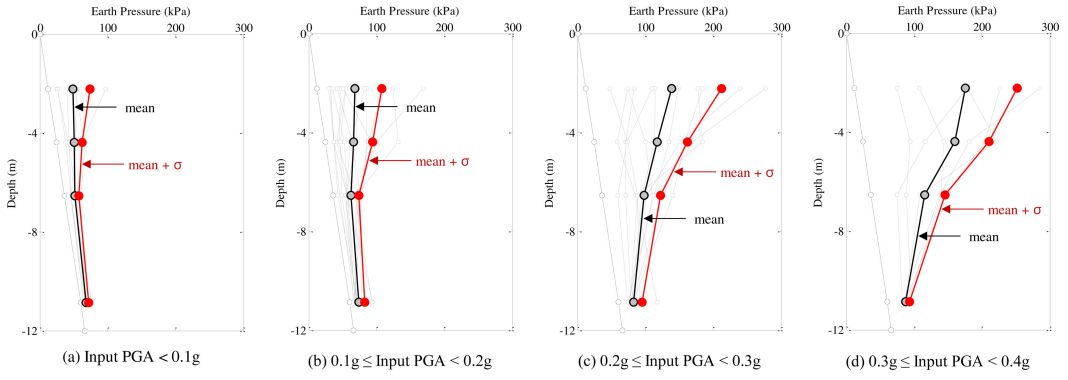

Figure 8. Dynamic earth pressure profiles according to input peak accelerations.

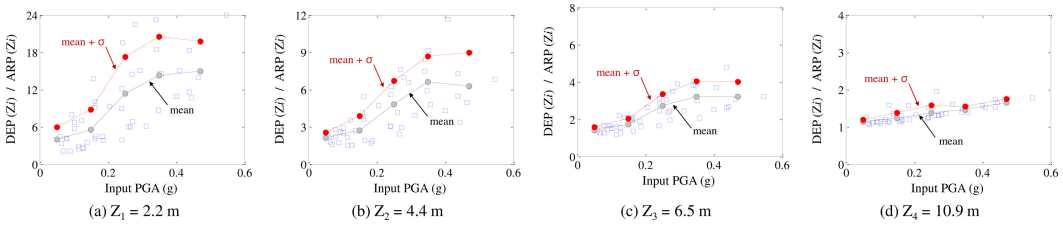

Figure 9. Ratio of dynamic earth pressure to at-rest earth pressure according to depth.

increases of the dynamic earth pressures near the surface were significantly greater than those near the bedrock, because the displacements of soil near the surface were greater than those near the bedrock.

5.3 *Ratio of dynamic earth pressure to at-rest earth pressure*

The dynamic earth pressure (DEP) acting on the basement at a point can be compared with the at-rest earth pressure (ARP) at the same point. Figure 9 shows ratios of the dynamic earth pressure to the at-rest earth pressure according to depth from surface.

As mentioned above, because the displacements of soil near the surface were large and the at-rest earth pressures near the surface were small, the ratios of the dynamic earth pressures to the at-rest earth pressures were greater than 15 at one fifth of the entire soil depth from the surface. On the other hand, the displacements of soil near the bedrock were small and the at-rest earth pressures near the bedrock were large, the ratios of the dynamic earth pressures to the at-rest earth pressures were smaller than 2 at five sixths of the entire soil depth from surface.

6 CONCLUSION

In the present study, to investigate the effect of soil-basement interaction on the earthquake responses of structures, centrifuge tests were performed. In 20 g, 40 g, and 60 g centrifugal accelerations, earthquakes were applied to the soil and structure by using an in-flight earthquake simulator at the bottom of soil container. Primary test variables were boundary conditions of basements and periods of structures. The results are summarized as follows.

1) Even though the lateral stiffness of the fixed basement was 3.75 times that of the soil deposit (FB1), the earthquake response of the basement depended on that of the massive soil deposit.
2) When half of the depth of the basement was embedded in the soil deposit, the embedded basement floated in the soil due to the large inertia force of the massive soil deposit.
3) Not only the ground motion but also the inertia force of the basement, which was in the forced vibration by the massive soil deposit, affected the earthquake response of structure. Thus, the seismic loads of the structures with periods similar to the site periods were amplified to 1.24∼1.61 times those of the fixed base structures.
4) The seismic loads of the structures on the half-embedded basement (EB1) were greater than those of the fixed base structures in whole period range.
5) When the maximum dynamic earth pressure acted on the front side of the basement during the earthquake, the earth pressures on the opposite side of the basement were diminished due to the gap between the soil and the basement.
6) Because the displacements of the soil near the surface were greater than the displacements of the soil near the bedrock, the dynamic earth pressures acting on the exterior wall, where designed for the small at-rest earth pressure, significantly increased.

REFERENCES

FEMA 440. 2004. Improvement of Nonlinear Static Seismic Analysis Procedures. *Federal Emergency Management Agency*, Washington, D.C.

Kim, D.S., Lee, S.H., Choo, Y.W., and Rames, D. 2013. Self-balanced earthquake simulator on centrifuge and dynamic performance verification. *KSCE Journal of Civil Engineering* 17(4):651–661.

Kim, N.R. & Kim, D.S. 2010. A Shear Wave Velocity Tomography System for Geotechnical Centrifuge Testing, *Geotechnical Testing Journal* 33:434–444.

Kim, S.S. 2007. High-Rise Building and Site Coefficient. *Architectural Structure (KSEA)* 14:73–78.

Kim, D.S. & Yoon, J.K. 2006. Development of New Site Classification System for the Regions of Shallow Bedrock in Korea, *Journal of Earthquake Engineering* 10:331–358.

Kramer, S.L. 1996. Geotechnical Earthquake Engineering, *Prentice Hall*, Upper Saddle River, NJ.

Lee, S.H., Choo, Y.W., and Kim, D.S. 2013. Performance of an equivalent shear beam (ESB) model container for dynamic geotechnical centrifuge tests. *Soil Dyn. Earthquake Eng.* 44(1):102–114.

Zeng, X. & Schofield, A.N. 1996. Design and Performance of an Equivalent Shear Beam (ESB) Container for Earthquake Centrifuge Modeling. *Geotechnique* 46(1):83–102.